analytical chemistry

pubs.acs.org/ac Article

Signal-On Mass Spectrometric Biosensing of Multiplex Matrix Metalloproteinases with a Phospholipid-Structured Mass-Encoded Microplate

Junjie Hu,[§] Fei Liu,[§] Yunlong Chen, Jia Fu, and Huangxian Ju*

Cite This: https://doi.org/10.1021/acs.analchem.3c01039 Read Online

ACCESS | Metrics & More | Article Recommendations | Supporting Information

ABSTRACT: The detection of matrix metalloproteinases (MMPs) is of great importance for diagnosis and staging of cancer. This work proposed a signal-on mass spectrometric biosensing strategy with a phospholipid-structured mass-encoded microplate for assessment of multiplex MMP activities. The designed substrate and internal standard peptides were subsequently labeled with the reagents of isobaric tags for relative and absolute quantification (iTRAQ), and DSPE-PEG(2000)-maleimide was embedded on the surface of a 96-well glass bottom plate to fabricate the phospholipid-structured mass-encoded microplate, which offered a simulated environment of the extracellular space for enzyme reactions between MMPs and the substrates. The strategy achieved multiplex MMP activity assays by dropping the sample in the well for enzyme cleavages, followed by adding trypsin to release the coding regions for ultrahigh performance liquid chromatography−tandem mass spectrometric (UHPLC−MS/MS) analysis. The peak area ratios of released coding regions and their respective internal standard (IS) peptides exhibited satisfied linear ranges of 0.05−50, 0.1−250, and 0.1−100 ng mL^{-1} with the detection limits of 0.017, 0.046, and 0.032 ng mL^{-1} for MMP-2, MMP-7, and MMP-3, respectively. The proposed strategy demonstrated good practicability in inhibition analysis and detections of multiplex MMP activities in serum samples. It is of great potential for clinical applications and can be expanded for multiplex enzyme assays.

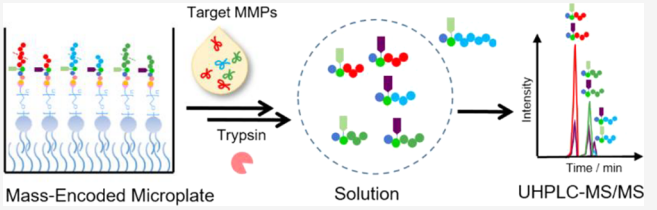

INTRODUCTION

Matrix metalloproteinases (MMPs) comprise a family of zinc-dependent proteinases, which participate in the degradation of the extracellular matrix (ECM), a three-dimensional network consisting of macromolecules and minerals for providing structural and biomedical support to the surrounding cells.[1−5] Under normal physiological conditions, different MMP members interact with specific ECM components, and their activities are precisely regulated at the level of activation and inhibition, respectively.[6,7] The activations of MMPs are significantly increased in human cancers compared with normal tissues and can promote cancer progression by increasing cancer-cell growth, migration, invasion, metastasis, and angiogenesis.[8−10] Thus, comprehensive activity assays of multiplex MMPs are very important and informative for auxiliary staging diagnosis of cancer and objective assessment of disease progression.

A variety of methods for analyzing MMP activities have been developed. Zymography is a commercial gel electrophoresis-based method for qualitative or semiquantitative analysis of a single sample, in which the substrates of MMPs are copolymerized in sodium dodecyl sulfate (SDS) polyacrylamide gel, and different MMPs can be separated based on the molecular weights.[11,12] Other methods such as colorimetric,[13−15] fluorescence,[16−18] bioluminescence,[19] surface-enhanced Raman scattering (SERS),[20] and electrochemical biosensors[21,22] are mainly cleavage-based strategies with substrate peptide probes, which are designed for specific interrogations of individual MMP activity in most cases. Some array-based[23,24] and logical[25] methods have been proposed for multiplex assay. However, due to the scarcity of tagging molecules, signal overlapping, as well as the complexity of data interpretation, the capacity of multiplex detections is seriously restricted.[26,27]

In order to overcome the bottleneck for multiplex enzyme activity assays, our group proposed "mass spectrometric biosensing" as a powerful tool for multiplex analysis with mass-tag probes, which could transfer the target information to explicit mass spectrometric signals.[28] This idea was successfully applied to the detection of MMP activities with a mass-encoded suspension array by ultrahigh performance liquid chromatography−tandem mass spectrometry (UHPLC−MS/MS).[29] The proposed method made use of the relative

Received: March 8, 2023
Accepted: May 15, 2023

Scheme 1. (A) Schematic Illustration of the Synthesis of DSPE-Substrate Peptides and DSPE-IS Peptides; (B) Mass-Encoded Microplate and Detection Procedure of Multiplex MMP Activities by UHPLC−MS/MS with the MRM Mode

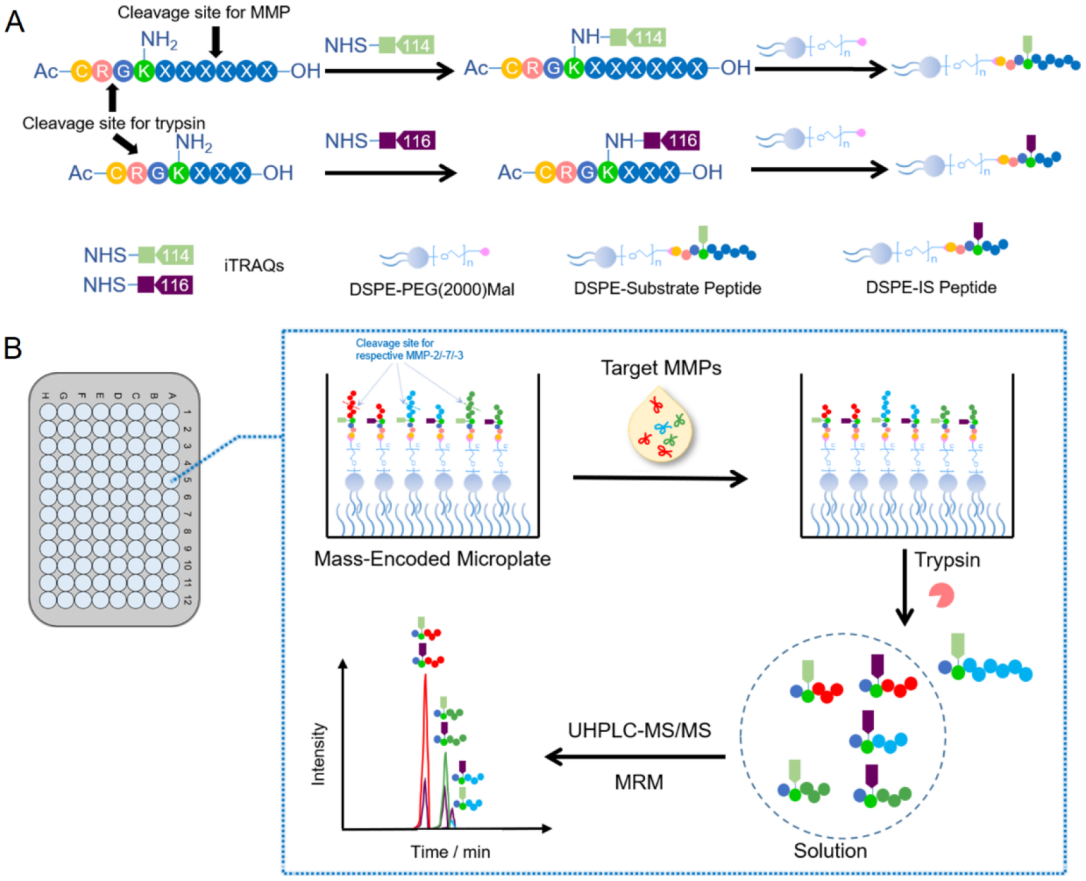

decrease of peak area ratios of coding regions to detection target MMP-2 and MMP-7 activities. Nonetheless, the "signal-off" biosensing strategy generally encounters uncertain signal loss of targets in heterogeneous clinical samples.[30] Thus, after fully considering the advantages of the peptide coding method[29,31,32] and the phospholipid-structured chip proposed previously,[33] this work designed different substrate peptide sequences and hydrophobic mass-encoded microplate to propose a "signal-on" biosensing mechanism for multiplex MMP activity assay.

The each substrate peptide was designed to sequentially contain a cleavage site for trypsin at the C-terminal of arginine (R) residue, lysine (K) with $-NH_2$ on the side chain to label isobaric tags for relative and absolute quantification (iTRAQ), and a substrate region for recognition and cleavage of the target MMP, while the sequence of the related internal standard (IS) peptide did not contain the cleavage site for MMPs (Scheme 1A). After the substrate and IS peptides were labeled with iTRAQs, they were conjugated with DSPE-PEG(2000)maleimide to obtain DSPE-substrate peptides and DSPE-IS peptides, respectively, and embedded on the hydrophobic surface of the 96-well glass bottom plate to get the mass-encoded microplate (Scheme 1). The assay could be performed by dropping the sample into the well for target MMP-2, MMP-7, and MMP-3 cleavages, followed by adding trypsin to release the coding regions for UHPLC−MS/MS analysis under a multiple reaction monitoring (MRM) mode. The detection of multiplex MMP activities was performed with the peak area ratios of released coding regions and their respective IS peptides (Scheme 1B). Compared with the previous strategy,[29] the innovations of this proposed method mainly manifested in two aspects: (i) the "signal-on" biosensing mechanism, which was different from previous "signal-off" mechanism and could increase the reliability and sensitivity for detections and simplify the processes for signal interpretations; (ii) the carrier of the 96-well glass bottom plate, with which the phospholipid-structured microplate could be efficiently constructed to create an extracellular-like space similar to the natural environment for the reactions between MMPs and the substrates. Thus, it supplied a great solution for multiplex MMP assays and was of great potential in accurate cancer diagnosis.

EXPERIMENTAL SECTION

Preparation of the Mass-Encoded Microplate. Hydrophobic modification of the 96-well plate, peptide labeling with iTRAQ reagents, and synthesis of DSPE-PEG(2000)-peptide conjugates (DP1−DP6) are described in the Supporting Information. The peptide sequences are listed in Table S1. To fabricate the phospholipid-structured mass-encoded microplate, 16 μL of the obtained DP1, DP3, and DP5, and 4 μL of ISs for DP2, DP4, and DP6 was dropped in a well of the 96-well plate, respectively, to incubate overnight at 4 °C. The DPs were immobilized on the glass surface through noncovalent hydrophobic interaction. Each well was washed twice with 200 μL of water and thoroughly dried with N_2 flow to obtain the mass-encoded microplate.

https://doi.org/10.1021/acs.analchem.3c01039
Anal. Chem. XXXX, XXX, XXX−XXX

As a comparison, gold foil (diameter 5 mm) was stuck on the bottom of each well, and 16 μL of P1-iTRAQ114, P3-iTRAQ114, and P5-iTRAQ114 and 4 μL of P2-iTRAQ116, P4-iTRAQ116, and P6-iTRAQ116 were added to each well of the plate to incubate overnight at 4 °C for covalently binding through Au−S bonds. The wells were subsequently washed twice with water and dried for further use.

UHPLC−MS/MS Analysis. UHPLC−MS/MS measurements were performed on an LC30A UHPLC system (Shimadzu, Japan) coupled with a QTRAP 5500 mass spectrometer (AB Sciex, USA). The samples (2 μL) were injected and separated on a Kinetex Biphenyl 100 Å column (100 × 3.0 mm, 2.6 μm, Phenomenex, USA) held at 40 °C. Mobile phase A was 5 mM NH_4OAc containing 0.1% formic acid, and mobile phase B was methanol containing 0.1% formic acid. The elution gradients were applied at the constant flow rate of 0.4 mL min^{-1} for a total run of 5.0 min: 0.0−1.0 min 5% B, 1.0−1.1 min 5−20% B, 1.1−2.0 min 20−95% B, 2.0−4.2 min 95% B, 4.2−4.3 min 95−5% B, 4.3−5.0 min 5% B, 5.0 min Stop. A 5500 QTRAP mass spectrometer with an electrospray ionization (ESI) source was operated in the positive MRM mode, with acquisition parameters such as curtain gas (30), ionspray voltage (5500), ion source gas 1 (45), ion source gas 2 (30), source temperature (550 °C), collision gas (High), declustering potentials (90), entrance potential (10), and collision cell exit potential (12). The ion transitions and optimized collision energies for peptide analytes are shown in Table 1. The dwell time was 100 ms for each transition. Data analysis was performed with Analyst and MultiQuant from AB Sciex (USA).

Table 1. Sequences and Optimized MRM Parameters for Coding Regions of MMP Cleavage Peptide Products and Their Respective Internal Standard Peptides

peptide name	sequence	charge	transition	collision energies
pP_{MMP-2}	GK(iTRAQ114) PLG	2	308.9/114.1	32
IS-pP_{MMP-2}	GK(iTRAQ116) PLG	2	308.9/116.1	32
pP_{MMP-7}	K(iTRAQ114) PRPLA	2	414.0/114.1	35
IS-pP_{MMP-7}	K(iTRAQ116) PRPLA	2	414.0/116.1	35
pP_{MMP-3}	GK(iTRAQ114) PYA	2	340.9/114.1	35
IS-pP_{MMP-3}	GK(iTRAQ116) PYA	2	340.9/116.1	35

Multiplex MMP Activity Assays. To perform qualitative and quantitative assays of MMP activities, 20 μL of samples, including MMP-2, MMP-7, MMP-3, and their mixtures at a series of concentrations (0−100 ng mL^{-1} for MMP-2, 0−500 ng mL^{-1} for MMP-7, and 0−200 ng mL^{-1} for MMP-3), MMP pre-mixed with the inhibitor batimastat (0−200 nM), or 5-fold diluted human serum samples with TCNB buffer (50 mM Tris−HCl, pH 7.6, 150 mM NaCl, 5 mM $CaCl_2$, and 0.05% Brij) were added to single wells of the mass-encoded microplate, respectively, to incubate at 37 °C for 2 h for target MMP cleavages. After removing the sample solutions and washing the well twice with 200 μL of water, 100 μL of 100 ng mL^{-1} trypsin in 25 mM NH_4HCO_3 was dropped to each well to incubate for 30 min for releasing the coding regions of MMP cleavage peptide products (pP_{MMP-2}, pP_{MMP-7}, and pP_{MMP-3}) and their respective IS peptides (IS-pP_{MMP-2}, IS-pP_{MMP-7}, and IS-pP_{MMP-3}) (Table 1). The obtained solutions were diluted to 5-fold volume with methanol containing 1% formic acid and subsequently subjected to UHPLC−MS/MS analysis.

RESULTS AND DISCUSSION

Fabrication of the Mass-Encoded Microplate. The hydrophobic glass substrate was first prepared via classical one-step C18-silanization with trimethoxy(octadecyl)silane (OTMS) for the fabrication of the mass-encoded microplate, which led to a contact angle change from 16.0° to 76.6° (Figure S1A,B). Meanwhile, DP1−DP6 were synthesized by labeling the peptides with iTRAQ reagents, which were demonstrated from the MALDI-MS spectra with a mass shift of +144 Da (Figure S2), and then conjugating the iTRAQ reagent-labeled peptides to DSPE-PEG(2000)maleimide. The mass spectra of DP1−DP6 showed the components at different m/z (Figure S3), as predicted in Table S1. Compared with DSPE-PEG(2000)maleimide (Figure S4), the results demonstrated the successful conjugation. The immobilization of DP1−DP6 on the 96-well plate was achieved through hydrophobic interaction, which led to contact angle change from 76.6° to 38.5° (Figure S1C). The energy dispersive spectroscopic (EDS) mapping analyses also showed the increasing elemental intensities and uniform distributions of C and P (Figure S1D−F), further confirming successive C18-silanization and assembly of DPs on the surfaces. The phospholipid layer structure on the well surface of the mass-encoded microplate provided an environment that is similar to that of the cell membrane or the extracellular space for the reaction of MMPs and corresponding substrates.[34,35]

Feasibility of Mass Spectrometric Biosensing. The feasibility of the proposed mass spectrometric biosensing strategy was tested by adding blank buffer, MMP-2, MMP-7, MMP-3, or their mixture to the wells of the mass-encoded microplate, respectively, to incubate at 37 °C for 2 h. Any concentrations of targets in the detection ranges could be selected to demonstrate the feasibility for simultaneous detections. Here, we chose single target samples of 50 ng mL^{-1} MMP-2, 125 ng mL^{-1} MMP-7, or 100 ng mL^{-1} MMP-3, as well as their mixtures containing multiplex targets to examine the performance of the proposed method. After each well was washed and subsequently digested with trypsin, the obtained solution was diluted and subjected for UHPLC−MS/MS analysis. The extracted MRM chromatograms showed three peaks at 2.84, 3.10, and 3.00 min, corresponding to the coding regions of MMP-cleaved product peptides and their respective IS peptides (2.84 min for pP_{MMP-2} and IS-pP_{MMP-2}, 3.10 min for pP_{MMP-7} and IS-pP_{MMP-7}, and 3.00 min for pP_{MMP-3} and IS-pP_{MMP-3}), respectively (Figure 1A−E). As predicted, blank TCNB buffer showed only IS-pP_{MMP}s on the extracted ion chromatograms (XICs) (Figure 1A), while the peak intensities for pP_{MMP-2}, pP_{MMP-7}, or pP_{MMP-3} individually increased in the presence of single target MMP-2, MMP-7, or MMP-3, respectively (Figure 1B−D), and simultaneously increased for the mixture of MMP-2, MMP-7, and MMP-3 (Figure 1E). Because the sequences of DP2, DP4, and DP6 did not include MMP substrate regions and only contained one cleavage site for trypsin, the released amounts of IS-pP_{MMP-2}, IS-pP_{MMP-7}, and IS-pP_{MMP-3} were constant in each well and rarely influenced by target MMPs, and thus, they could serve as internal standards to reduce the matrix effects for quantitative

https://doi.org/10.1021/acs.analchem.3c01039
Anal. Chem. XXXX, XXX, XXX−XXX

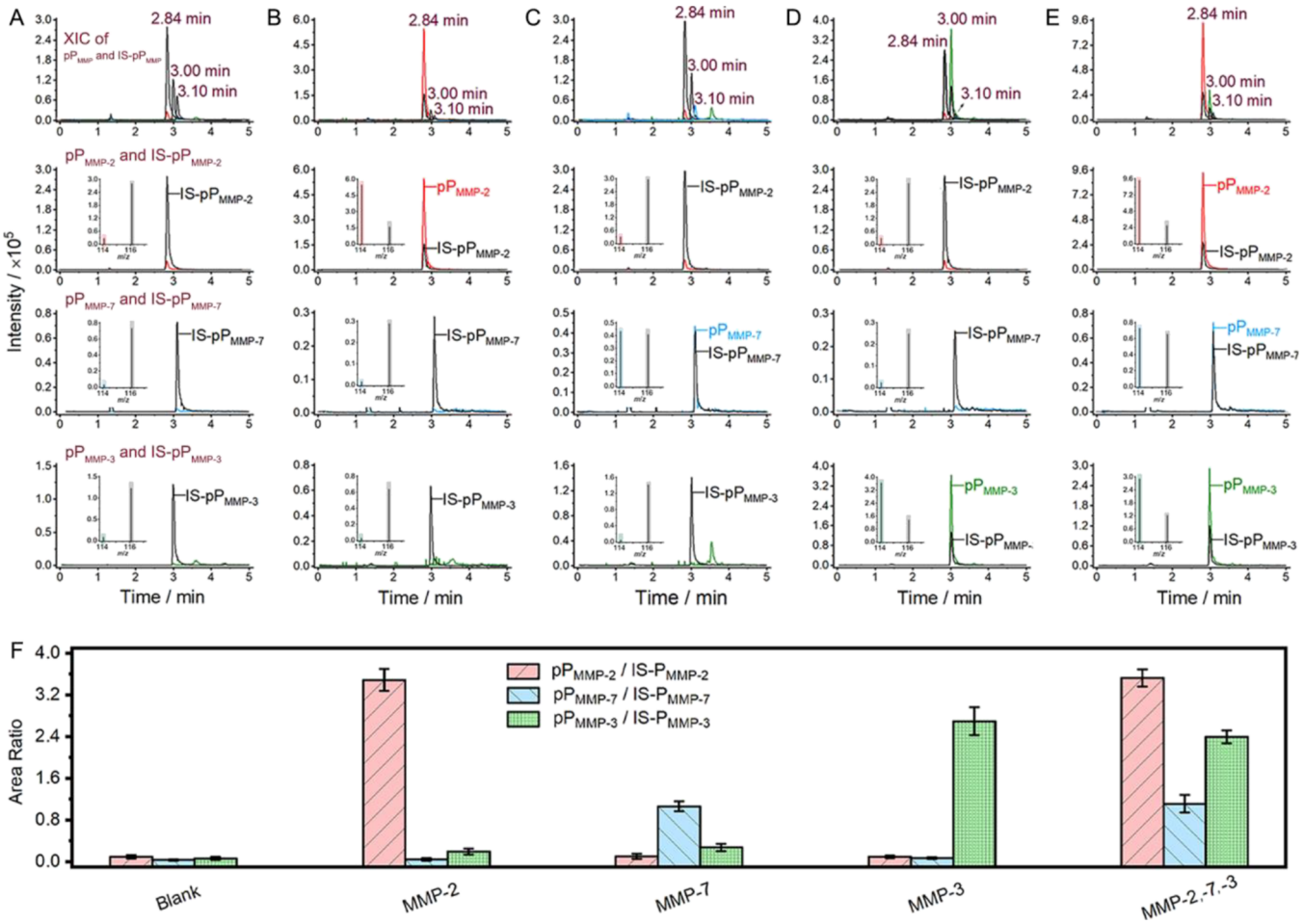

Figure 1. Extracted MRM chromatograms of released coding regions of the target MMP-cleaved products and their respective IS peptides by adding (A) blank buffer, (B) 50 ng mL^{-1} MMP-2, (C) 125 ng mL^{-1} MMP-7, (D) 100 ng mL^{-1} MMP-3, and (E) the mixture of 50 ng mL^{-1} MMP-2, 125 ng mL^{-1} MMP-7, and 100 ng mL^{-1} MMP-3 was placed into the wells of the mass-encoded microplate and incubated for 2 h and then treated with trypsin. Insets: MS/MS spectra of the detected tags of iTRAQ114 and iTRAQ116 for respective pP_{MMP}s and IS-pP_{MMP}s. (F) Peak area ratios of pP_{MMP-2}/IS-pP_{MMP-2}, pP_{MMP-7}/IS-pP_{MMP-7}, and pP_{MMP-3}/IS-pP_{MMP-3} for samples (A)−(E).

analysis. The peak area ratios of pP_{MMP-2}/IS-pP_{MMP-2}, pP_{MMP-7}/IS-pP_{MMP-7}, and pP_{MMP-3}/IS-pP_{MMP-3} showed dramatical increases with MMP-2, MMP-7, and MMP-3, respectively, and revealed little cross influence between different targets (Figure 1F), enabling simultaneous multiplex MMP activity assays with the mass-encoded microplate.

As a comparison, another plate was fabricated by directly immobilizing the iTRAQ-labeled peptides on the gold foil-sticked surface of the 96-well plate via Au−S binding, following the same experimental process for the detections of MMP activities. As shown in Figure S5, the peak intensities for pP_{MMP}s and IS-pP_{MMP}s were less than 5% of the peak intensities in Figure 1E, and each peak area ratio of pP_{MMP}/IS-pP_{MMP} was also lower than that displayed in Figure 1F. It probably resulted from the lower amounts of covalently immobilized iTRAQ-labeled peptides and the lower cleavage efficiencies of peptide-iTRAQs with targets. This result demonstrated the advantages of efficient substrate immobilization through non-covalent interaction and the simulated natural environment for MMP cleavage reactions, further proving the superiorities of the phospholipid-structured mass-encoded microplate.

Quantitative Detections of Multiplex MMP Activities. The effect of trypsin concentration was examined to ensure complete releases of coding regions of MMP cleavage peptide products and their respective ISs. All of the peak areas of pP_{MMP-2}, pP_{MMP-7}, pP_{MMP-3}, IS-pP_{MMP-2}, IS-pP_{MMP-7}, and IS-pP_{MMP-3} reached the maximum at a trypsin concentration of 100 ng mL^{-1} (Figure S6), suggesting the maximum releases of all the coding regions. The incubation time was also optimized by dropping the mixture of MMP-2, MMP-7, and MMP-3 in the wells to incubate for different times. The peak area ratios of pP_{MMP-2}/IS-pP_{MMP-2}, pP_{MMP-7}/IS-pP_{MMP-7}, and pP_{MMP-3}/IS-pP_{MMP-3} trended the plateaus at 120 min, indicating the completion of enzyme cleavages (Figure S7). Thus, the MMP incubation time of 120 min and the trypsin concentration of 100 ng mL^{-1} were adopted for quantitative analysis.

Upon the optimized conditions, the mixtures of MMP-2, MMP-7, and MMP-3 at different series of concentrations were added in the wells of the mass-encoded microplate to perform quantitative detections of multiplex MMP activities. Their extracted MRM chromatograms showed that the peak intensities of pP_{MMP-2}, pP_{MMP-7}, and pP_{MMP-3} increased with increasing concentrations of MMP-2, MMP-7 and MMP-3, respectively (Figure 2A−C). The plots of the peak area ratios of pP_{MMP-2}/IS-pP_{MMP-2}, pP_{MMP-7}/IS-pP_{MMP-7}, and pP_{MMP-3}/IS-pP_{MMP-3} versus the concentrations of MMP-2, MMP-7, and MMP-3 displayed satisfied linearity in the ranges of 0.05−50,

https://doi.org/10.1021/acs.analchem.3c01039
Anal. Chem. XXXX, XXX, XXX−XXX

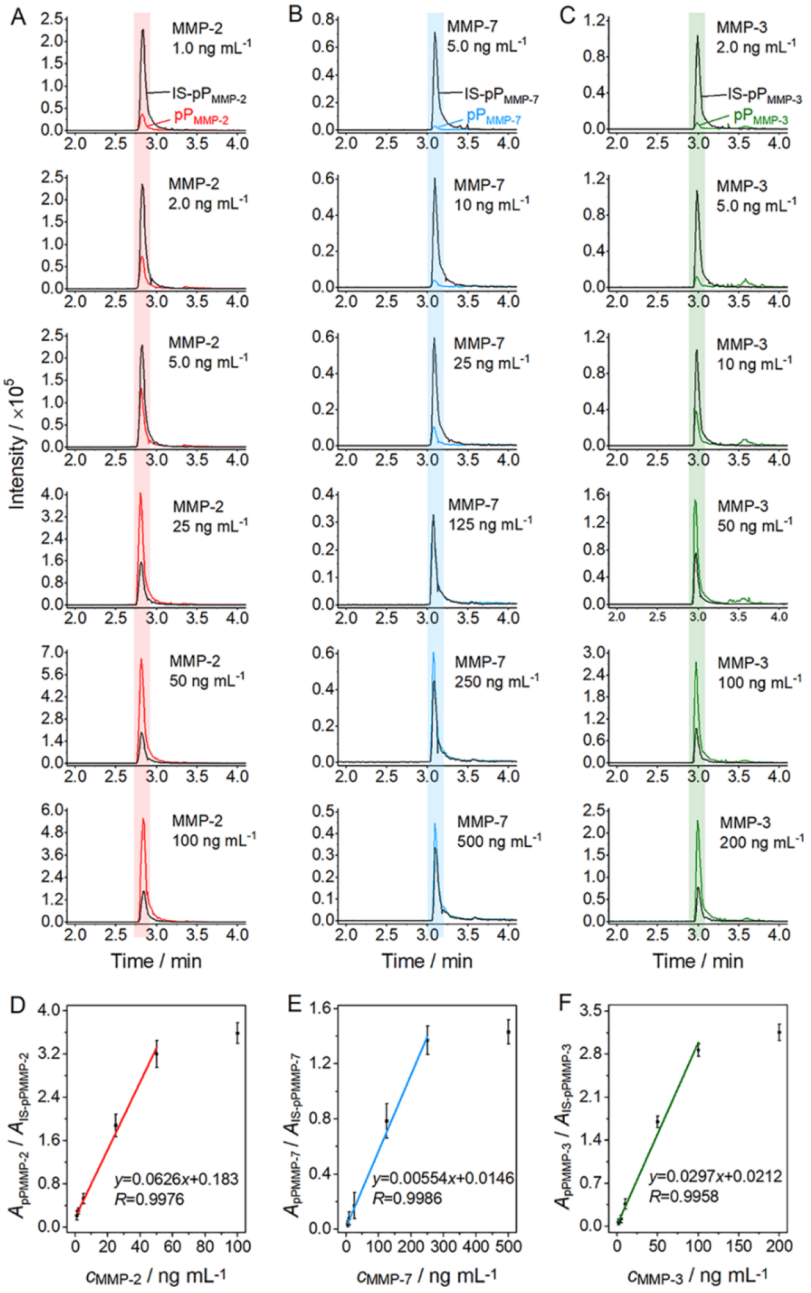

Figure 2. Extracted MRM chromatograms of (A) pP_{MMP-2} and IS-pP_{MMP-2}, (B) pP_{MMP-7} and IS-pP_{MMP-7}, and (C) pP_{MMP-3} and IS-pP_{MMP-3} by adding the mixture of MMP-2, MMP-7, and MMP-3 at a series of concentrations and then treating with trypsin. Plots of peak area ratios of (D) pP_{MMP-2}/IS-pP_{MMP-2}, (E) pP_{MMP-7}/IS-pP_{MMP-7}, and (F) pP_{MMP-3}/IS-pP_{MMP-3} vs MMP-2, MMP-7, and MMP-3 concentrations.

0.1−250, and 0.1−100 ng mL^{-1} with $R > 0.995$, respectively (Figure 2D−F). The detection limits for MMP-2, MMP-7, and MMP-3 at 3σ were 0.017, 0.046, and 0.032 ng mL^{-1}, respectively, which were lower than the reported values with the signal-off mass spectrometric biosensing method[29] and were comparable with those reported with other methods, such as electrochemical, fluorescence, and MS detections (Table S2).

Specificity, Reproducibility, and Stability. The specificity of the proposed method was evaluated with interferential enzymes or proteins. The peak area ratios of pP_{MMP-2}/IS-pP_{MMP-2}, pP_{MMP-7}/IS-pP_{MMP-7}, and pP_{MMP-3}/IS-pP_{MMP-3} for their respective targets of MMP-2, MMP-7, and MMP-3 were 5−20 folds higher than that of the blank, while the ratios for interferential substances of MMP-1, caspase-3, caspase-8, and bovine serum albumin (BSA) were close to that of the blank (Figure S8), indicating good specificity of the proposed strategy.

The reproducibility was investigated with inter-assay and intra-assay tests. The inter-assay tests were performed by adding the mixture of 25 ng mL^{-1} MMP-2, 125 ng mL^{-1} MMP-7, and 50 ng mL^{-1} MMP-3 to six wells on the mass-encoded microplate independently to measure the mass spectrometric responses, which showed the maximum relative standard deviation (RSD) of 4.3%. The intra-assay tests were performed by submitting one of the samples for UHPLC MS/MS analysis for six times, which showed the RSDs less than 5.0% (Figure S9A). The stability of the mass-encoded

https://doi.org/10.1021/acs.analchem.3c01039
Anal. Chem. XXXX, XXX, XXX−XXX

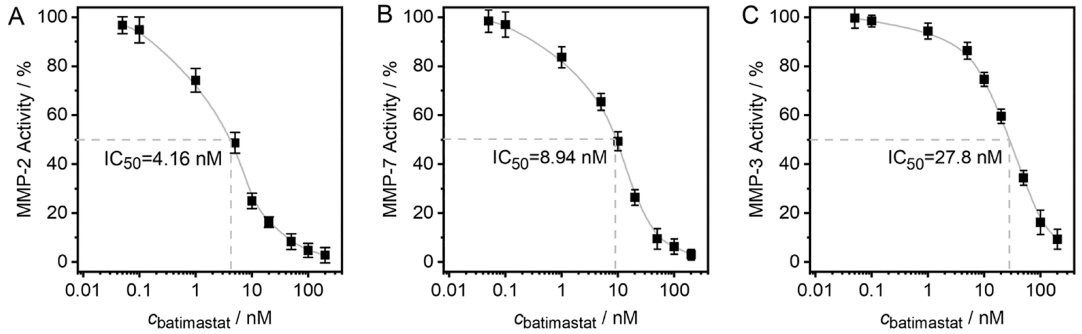

Figure 3. Plots of the activities of (A) 50 ng mL^{-1} MMP-2, (B) 125 ng mL^{-1} MMP-7, and (C) 100 ng mL^{-1} MMP-3 vs logarithm of batimastat concentration.

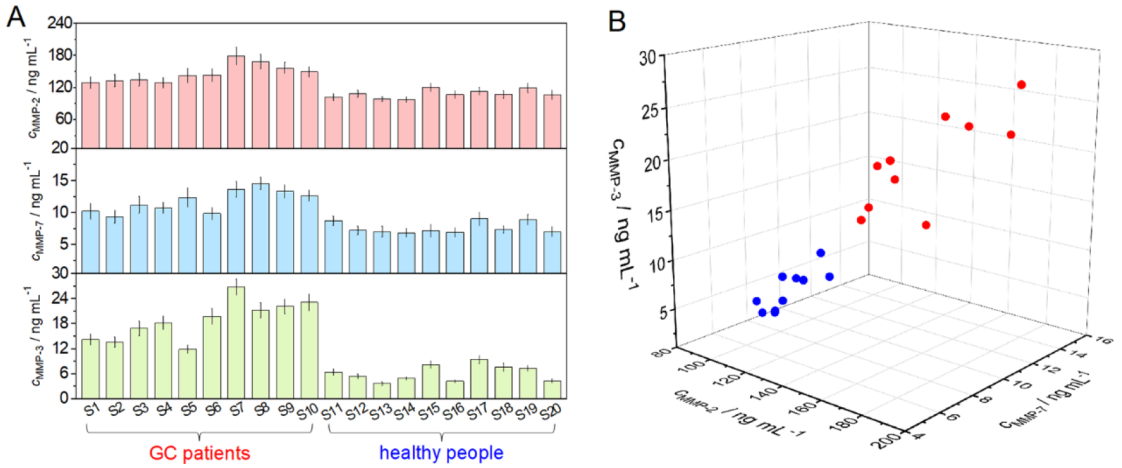

Figure 4. (A) Activity of MMP-2, MMP-7, and MMP-3 in human serum samples from ten GC patients and ten healthy people determined with the mass-encoded microplate. (B) Three dimensional scatter profile of MMP-2, MMP-7, and MMP-3 activities in serum samples (A).

microplate was examined by storing it at 4 °C for 7 and 28 days. The peak area ratios of pP_{MMP-2}/IS-pP_{MMP-2}, pP_{MMP-7}/IS-pP_{MMP-7}, and pP_{MMP-3}/IS-pP_{MMP-3} for target MMP activity assays at the same concentration did not obviously change (Figure S9B). These results demonstrated acceptable reproducibility and stability of the prepared device.

MMP Inhibitor Analysis. The proposed mass spectrometric biosensing strategy was used to evaluate the inhibition effect of MMP inhibitor batimastat on their activities. After pre-mixing MMP-2, MMP-7, and MMP-3 with batimastat, the peak intensities of pP_{MMP-2}, pP_{MMP-7} and pP_{MMP-3}, and the ratios of pP_{MMP-2}/IS-pP_{MMP-2}, pP_{MMP-7}/IS-pP_{MMP-7}, and pP_{MMP-3}/IS-pP_{MMP-3} exhibited a sharp decline compared to those in the absence of this inhibitor (Figure S10), suggesting significant decreases in MMP activities. The IC_{50} values (50% inhibition efficiency) of batimastat for MMP-2, MMP-7, and MMP-3 were estimated to be 4.16, 8.94, and 27.8 nM, respectively (Figure 3), which were quite close to the reported 4 nM, 6 nM, and 20 nM, respectively.[36] The results demonstrated the practical application in the screening of MMP inhibitors with the mass-encoded microplate.

Clinical Serum Sample Analysis. To assess the performance of the proposed method in the prediction and diagnosis of cancer, the experiments for simultaneous detection of MMP-2, MMP-7, and MMP-3 activities in human serum samples from gastric cancer (GC) patients and healthy people (for clinical information of each sample, see Table S3) were performed with the mass-encoded microplate. Considering MMP-2, -7 and -3 levels in human serum, linear ranges and matrix interferences, all the samples were diluted to 5-fold volumes with TCNB buffer. The obtained concentrations of MMP-2, MMP-7, and MMP-3 in the samples from GC patients were higher than those from healthy people (Figure 4A). The average levels of MMP-2, MMP-7, and MMP-3 from ten GC patients were 146.8, 11.81, and 18.80 ng mL^{-1}, which were visibly higher than those of 108.3, 7.66, and 6.13 ng mL^{-1} from ten healthy people, respectively. The three-dimensional (3D) scatter diagram also showed an obvious aggregation tendency (Figure 4B). It should be noted that the activities of MMP-2, MMP-7, and MMP-3 in serum samples were closely related with whether the tumor has spread and broadly increased with the stage of GC patients (Figure S11).[37−39] The results indicated potential application of this strategy for diagnosis and staging of cancer.

To further evaluate the reliability of the mass spectrometric biosensing strategy, the recoveries of MMP-2, MMP-7, and MMP-3 were measured by spiking them at different concentrations in 5-fold diluted S10 and S20. All recoveries were between 90.2−98.1% (Table S4). The assay results with the proposed mass spectrometric biosensing method were also compared with those obtained by the ELISA kits, which showed the relative errors in the range of −7.48 to 2.37% (Table S4), suggesting acceptable accuracy for multiplex MMP activity assays in clinical samples.

https://doi.org/10.1021/acs.analchem.3c01039
Anal. Chem. XXXX, XXX, XXX−XXX

CONCLUSIONS

This work proposes a "signal-on" mass spectrometric biosensing strategy with a phospholipid-structured mass-encoded microplate. The microplate was fabricated by embedding the iTRAQ-labeled DSPE-PEG(2000)-substrate and IS peptides on the surface of a 96-well plate through hydrophobic interaction, which creates a simulated natural environment of extracellular space for the reactions between MMPs and substrates. The assay can be simply performed by dropping the sample into the well for target MMP cleavage and then adding trypsin to release the coding regions for UHPLC−MS/MS quantitative analysis with the peak area ratios of coding regions of MMP cleavage peptide products and their respective IS peptides. This strategy shows excellent performance with wide concentration ranges and high sensitivity and can be used for inhibition analysis and MMP activity assays in human serum samples, demonstrating great potential in drug screening and accurate diagnosis of cancer. The mass spectrometric biosensing strategy and the mass-encoded microplate provide a new approach for multiplex enzyme activity assays with high sensitivity and good specificity. The mass-tag probes are also of potential applications in other types of mass spectrometry platforms, such as MALDI-TOF MS.[40] By more elaborately designing the substrate sequences, this method can be expanded for simultaneous and accurate multiplex assays of other enzyme activities in various physiological processes.

ASSOCIATED CONTENT

Supporting Information

The Supporting Information is available free of charge at https://pubs.acs.org/doi/10.1021/acs.analchem.3c01039.

Materials and reagents, additional experimental details, contact angles and EDS mapping of the glass surface, MALDI-TOF mass spectra of the peptides, peptide-iTRAQ conjugates, DSPE-PEG(2000)maleimide, and DP1−DP6, extracted MRM chromatograms for gold foil-sticked microplate, responses to the inhibitor, optimization of trypsin concentration and incubation time, specificity, reproducibility, and stability of the method, relations between serum MMP activities and GC processes, peptide sequences and molecular weights, comparison of different assay performance, clinical information of serum samples, recovery test results, and comparison of the assay results with ELISA method (PDF)

AUTHOR INFORMATION

Corresponding Author

Huangxian Ju − *State Key Laboratory of Analytical Chemistry for Life Science, School of Chemistry and Chemical Engineering, Nanjing University, Nanjing 210023, China;* orcid.org/0000-0002-6741-5302; Phone: +86-25-89683593; Email: hxju@nju.edu.cn; Fax: +86-25-89683593

Authors

Junjie Hu − *State Key Laboratory of Analytical Chemistry for Life Science, School of Chemistry and Chemical Engineering, Nanjing University, Nanjing 210023, China; College of Forensic Medicine and Laboratory Medicine, Jining Medical University, Jining 272067, China;* orcid.org/0000-0001-8976-3626

Fei Liu − *State Key Laboratory of Analytical Chemistry for Life Science, School of Chemistry and Chemical Engineering, Nanjing University, Nanjing 210023, China*

Yunlong Chen − *State Key Laboratory of Analytical Chemistry for Life Science, School of Chemistry and Chemical Engineering, Nanjing University, Nanjing 210023, China;* orcid.org/0000-0002-3775-3028

Jia Fu − *College of Forensic Medicine and Laboratory Medicine, Jining Medical University, Jining 272067, China*

Complete contact information is available at: https://pubs.acs.org/10.1021/acs.analchem.3c01039

Author Contributions

[§]J.H. and F.L. contributed equally to this work.

Notes

The authors declare no competing financial interest.

ACKNOWLEDGMENTS

This work was financially supported by the National Natural Science Foundation of China (21904049, 21827812, and 21974063), China Postdoctoral Science Foundation (2022M721553), and the Project of Shandong Province Higher Educational Youth Innovation Science and Technology Program (2022KJ106). We specially thank Dr. Bin Zhang and Jingxia Zheng in Department of Laboratory Medicine, Affiliated Hospital of Jining Medical University for providing serum samples used in the experiments.

REFERENCES

(1) de Almeida, L. G. N.; Thode, H.; Eslambolchi, Y.; Chopra, S.; Young, D.; Gill, S.; Devel, L.; Dufour, A. *Pharmacol. Rev.* **2022**, *74*, 714−770.

(2) Lei, Z.; Jian, M.; Li, X.; Wei, J.; Meng, X.; Wang, Z. *J. Mater. Chem. B* **2020**, *8*, 3261−3291.

(3) Mouw, J. K.; Ou, G.; Weaver, V. M. *Nat. Rev. Mol. Cell Biol.* **2014**, *15*, 771−785.

(4) Bonnans, C.; Chou, J.; Werb, Z. *Nat. Rev. Mol. Cell Biol.* **2014**, *15*, 786−801.

(5) Hussey, G. S.; Dziki, J. L.; Badylak, S. F. *Nat. Rev. Mater.* **2018**, *3*, 159−173.

(6) Laronha, H.; Caldeira, J. *Cell* **2020**, *9*, 1076.

(7) Zhou, J.; Wang, M.; Ying, H.; Su, D.; Zhang, H.; Lu, G.; Chen, J. *ACS Biomater. Sci. Eng.* **2018**, *4*, 2404−2411.

(8) Egelblad, M.; Werb, Z. *Nat. Rev. Cancer* **2002**, *2*, 161−174.

(9) Gong, T. X.; Kong, K. V.; Goh, D.; Olivo, M.; Yong, K. -T. *Biomed. Opt. Express* **2015**, *6*, 2076−2087.

(10) Jonsson, A.; Hjalmarsson, C.; Falk, P.; Ivarsson, M.-L. *Br. J. Cancer* **2016**, *115*, 703−706.

(11) Tajhya, R. B.; Patel, R. S.; Beeton, C. Detection of Matrix Metalloproteinases by Zympgraphy. In *Methods in Molecular Biology 1579: Matrix Metalloproteases Methods and Protocols*; Galea, C. A., Ed.; Humana Press: New York, NY, 2017; pp 231−244.

(12) Snoek-van Beurden, P. A. M.; Von den Hoff, J. W. *BioTechniques* **2005**, *38*, 73−83.

(13) Cheng, W.; Chen, Y.; Yan, F.; Ding, L.; Ding, S.; Ju, H.; Yin, Y. *Chem. Commun.* **2011**, *47*, 2877−2879.

(14) Nguyen, D. L.; Kim, H.; Kim, D.; Lee, J. O.; Gye, M. C.; Kim, Y. -P. *Sensors* **2018**, *18*, 875.

(15) Zhong, Z.-T.; Ashraf, G.; Chen, W.; Liu, B.; Wang, G.-P.; Zhao, Y.-D. *Anal. Chem.* **2022**, *94*, 16384−16392.

(16) Liu, L.; Chu, H.; Yang, J.; Sun, Y.; Ma, P.; Song, D. *Biosens. Bioelectron.* **2022**, *212*, No. 114389.

(17) Zeng, W.; Wu, L.; Sun, Y.; Wang, Y.; Wang, J.; Ye, D. *Small* **2021**, *17*, No. 2101924.
(18) Cao, S.; Li, Z.; Zhao, J.; Chen, M.; Ma, N. *ACS Sens.* **2018**, *3*, 1522−1530.
(19) Tian, F.; Chen, Y.; Wang, W.; Zhang, J.; Jiang, T.; Lu, Q. *Anal. Chem.* **2021**, *93*, 8739−8745.
(20) Zhong, Q.; Zhang, K.; Huang, X.; Lu, Y.; Zhao, J.; He, Y.; Liu, B. *Biosens. Bioelectron.* **2022**, *207*, No. 114194.
(21) Xi, X.; Wen, M.; Song, S.; Zhu, J.; Wen, W.; Zhang, X.; Wang, S. *Chem. Commun.* **2020**, *56*, 6039−6042.
(22) Duan, S.; Peng, J.; Cheng, H.; Li, W.; Jia, R.; Liu, J.; He, X.; Wang, K. *Talanta* **2021**, *231*, No. 122418.
(23) Lei, Z.; Zhang, H.; Wang, Y.; Meng, X.; Wang, Z. *Anal. Chem.* **2017**, *89*, 6749−6757.
(24) Jian, M.; Su, M.; Gao, J.; Wang, Z. *Sens. Actuators, B* **2020**, *304*, No. 127320.
(25) Gong, T.; Hong, Z.-T.; Chen, C.-H.; Tsai, C.-Y.; Liao, L.-D.; Kong, K. V. *ACS Nano* **2017**, *11*, 3365−3375.
(26) Jet, T.; Gines, G.; Rondelez, Y.; Taly, V. *Chem. Soc. Rev.* **2021**, *50*, 4141−4161.
(27) Rosa, B. G.; Akingbade, O. E.; Guo, X.; Gonzalez-Macia, L.; Crone, M. A.; Cameron, L. P.; Freemont, P.; Choy, K. -L.; Güder, F.; Yeatman, E.; Sharp, D. J.; Li, B. *Biosens. Bioelectron.* **2022**, *203*, No. 114050.
(28) Hu, J.; Liu, F.; Chen, Y.; Shangguan, G.; Ju, H. *ACS Sens.* **2021**, *6*, 3517−3535.
(29) Hu, J.; Liu, F.; Chen, Y.; Fu, J.; Shangguan, G.; Ju, H. *Anal. Chem.* **2022**, *94*, 6380−6386.
(30) Zhang, Z.; Sen, P.; Adhikari, B.; Li, Y.; Soleymani, L. *Angew. Chem., Int. Ed.* **2022**, *61*, No. e202212496.
(31) Hu, J.; Liu, F.; Ju, H. *Anal. Chem.* **2015**, *87*, 4409−4414.
(32) Hu, J.; Liu, F.; Feng, N.; Ju, H. *Anal. Chim. Acta* **2019**, *1064*, 1−10.
(33) Hu, J.; Liu, F.; Ju, H. *Angew. Chem., Int. Ed.* **2016**, *55*, 6667−6670.
(34) Sternlicht, M. D.; Werb, Z. *Annu. Rev. Cell Dev. Biol.* **2001**, *17*, 463−516.
(35) Shiomi, T.; Inoki, I.; Kataoka, F.; Ohtsuka, T.; Hashimoto, G.; Nemori, R.; Okada, Y. *Lab. Invest.* **2005**, *85*, 1489−1506.
(36) Laronha, H.; Carpinteiro, I.; Portugal, J.; Azul, A.; Polido, M.; Petrova, K. T.; Salema-Oom, M.; Caldeira, J. *Biomolecules* **2020**, *10*, 717.
(37) Kushlinskii, N. E.; Gershtein, E. S.; Ivannikov, A. A.; Davydov, M. M.; Chang, V. L.; Ognerubov, N. A.; Stilidi, I. S. *Bull. Exp. Biol. Med.* **2019**, *166*, 373−376.
(38) Shi, Y.; Su, C.; Hu, H.; Yan, H.; Li, W.; Chen, G.; Xu, D.; Du, X.; Zhang, P. *PLoS One* **2018**, *13*, No. e0198896.
(39) Liu, J.; Zhou, L.; Lin, S.; Yao, B. *Pak. J. Med. Sci.* **2020**, *36*, 1025−1031.
(40) Wang, Y.; Zhang, K.; Huang, X.; Qiao, L.; Liu, B. *Anal. Chem.* **2021**, *93*, 709−714.

https://doi.org/10.1021/acs.analchem.3c01039
Anal. Chem. XXXX, XXX, XXX−XXX